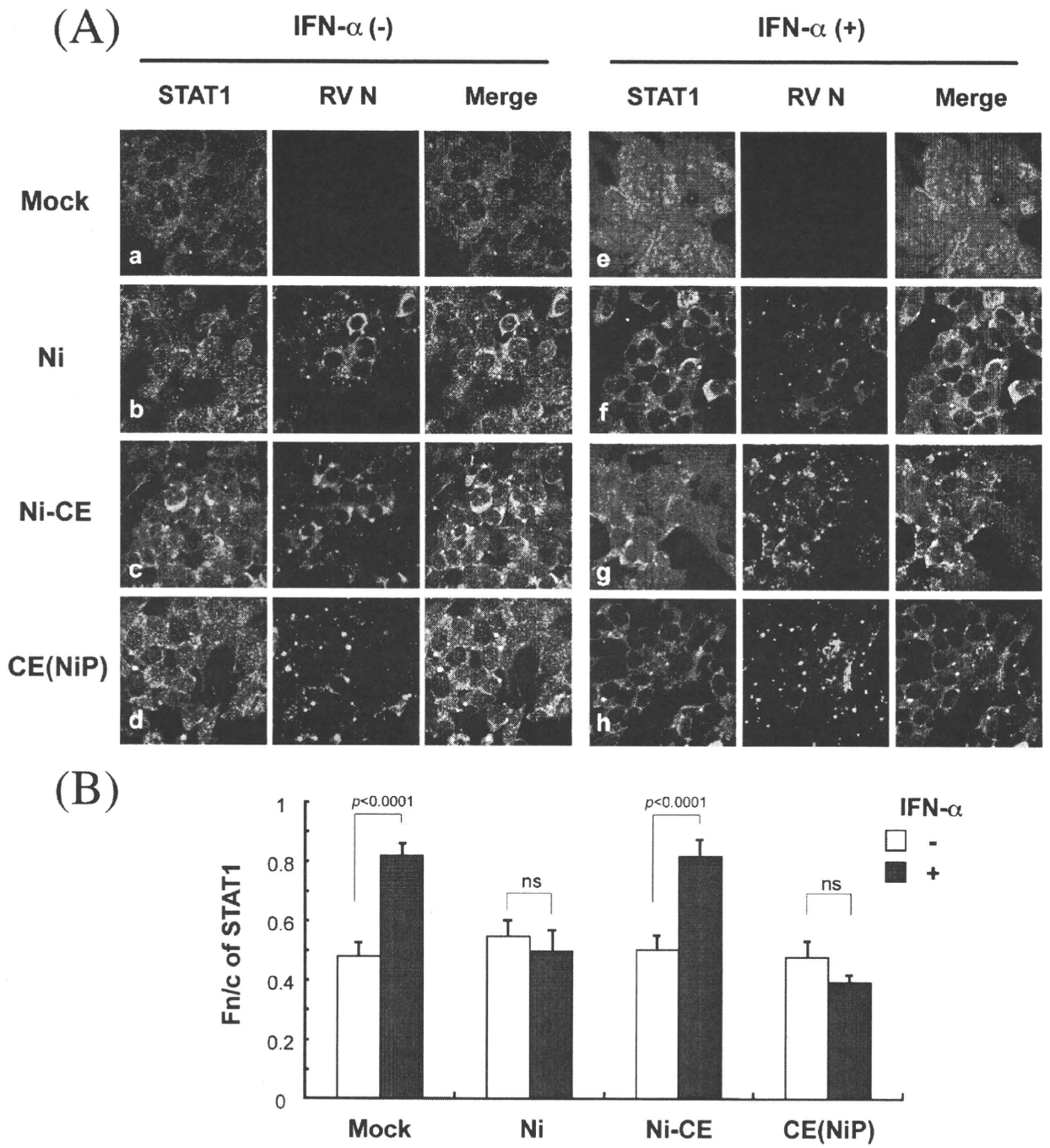

FIG. 4. The subcellular localization of STAT1 in RV-infected SK-N-SH cells differs between the viral strains. (A) The cells were inoculated with each strain at an MOI of 0.01 and then were treated with IFN-α (4,000 U/ml) for 30 min at 24 h p.i. The cells were fixed with 3.7% formaldehyde for 10 min and 90% methanol for 5 min before being immunostained for STAT1 (green) and RV N protein (red) and analyzed by CLSM. (B) Images such as those shown in panel A were used to calculate the ratios of nuclear to cytoplasmic fluorescence (Fn/c) of STAT1, which are shown as the means ± standard errors of the means of the results from >30 images. ns, not significant ($P \geq 0.05$); Ni, Nishigahara.

0.0001 and $P < 0.01$, respectively) (Fig. 3A and B), consistent with the results from the ISRE reporter assays. These results demonstrate that Nishigahara P protein blocks IFN signaling more efficiently than Ni-CE P protein.

Infection with the Nishigahara or CE(NiP) but not the Ni-CE strain effectively inhibits IFN-induced nuclear translocation of STAT1. The results of previous studies have indicated that the inhibitory effect of RV P protein on IFN signaling

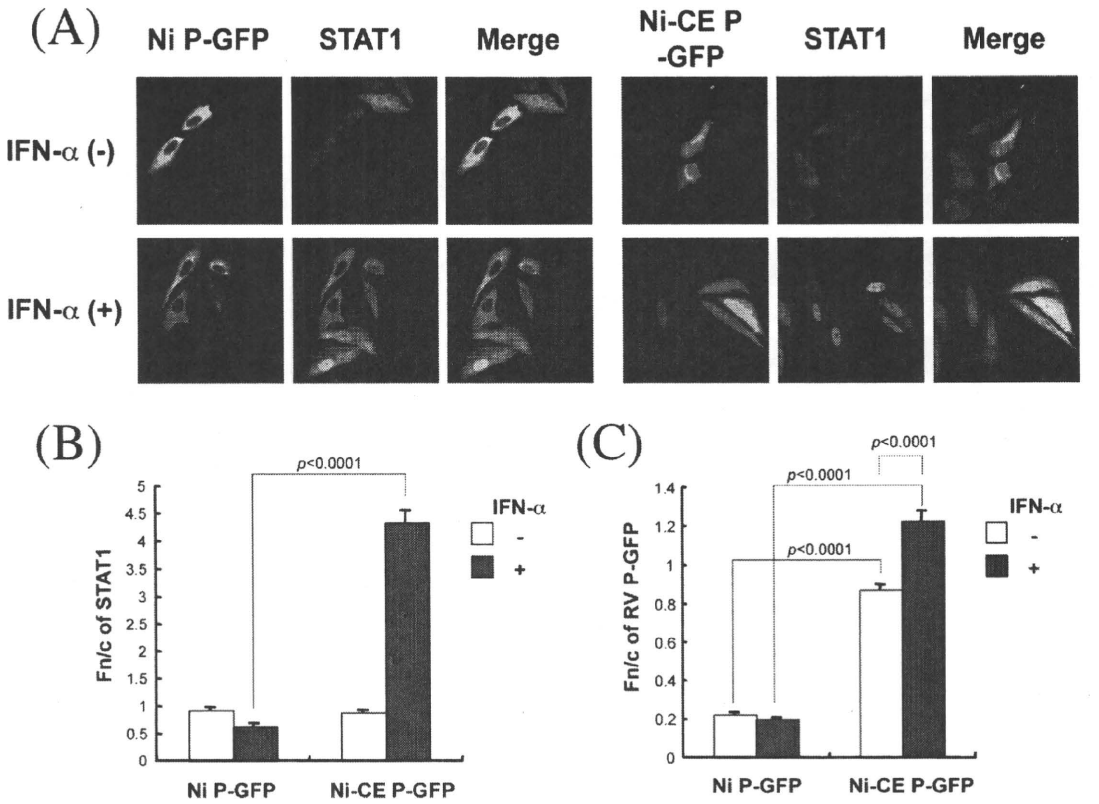

FIG. 5. The Ni-CE P protein is defective for cytoplasmic localization and for its capacity to inhibit nuclear import of IFN-activated STAT1. (A) Vero cells were transfected to express the indicated GFP-tagged P protein (green) and, 18 h later, were treated with or without IFN-α for 1 h. The cells were fixed with formaldehyde and methanol and immunostained for STAT1 (red) before being analyzed by CLSM. (B, C) Images such as those shown in panel A were analyzed to derive the ratio of nuclear to cytoplasmic fluorescence (Fn/c) values (mean ± standard error of the mean, $n > 130$, combined data from 3 separate assays) for STAT1 (B) or GFP-tagged P protein (C). Ni, Nishigahara.

depends on a physical interaction of the P protein with the IFN-activated transcription factor STAT1 (4, 36). The P protein-STAT1 interaction does not affect the activation (i.e., phosphorylation) of STAT1 but, rather, appears to block its nuclear translocation (36). However, the significance of this in viral pathogenicity has not been assessed. Accordingly, to investigate the possibility that Nishigahara P protein but not Ni-CE P protein effectively inhibits the nuclear translocation of STAT1, we examined STAT1 subcellular localization in Nishigahara-, Ni-CE-, and CE(NiP)-infected SK-N-SH cells (treated with or without IFN-α) by immunofluorescence assay followed by CLSM analysis (Fig. 4A). In mock-infected cells, STAT1 was localized mainly in the cytoplasm of IFN-α-untreated cells (Fig. 4A, a) but became localized in the nucleus after IFN-α treatment (Fig. 4A, e), indicating clear nuclear translocation of IFN-activated STAT1. In IFN-α-untreated, RV-infected cells, STAT1 was found to be mainly in the cytoplasm, regardless of the RV strain infected (Fig. 4A, b to d). Importantly, in IFN-α-treated cells, Nishigahara and CE(NiP) infections resulted in inhibition of STAT1 nuclear translocation (Fig. 4A, f and h, respectively), whereas Ni-CE infection had no apparent effect (Fig. 4A, g). Comparable results for phosphorylated STAT1 in infected SK-N-SH cells were obtained by immunostaining (data not shown).

To quantify these effects, we analyzed digitized CLSM images as previously reported (16, 17), to calculate the ratio of nuclear to cytoplasmic fluorescence (Fn/c), corrected for background fluorescence, of STAT1 in the infected cells. In IFN-α-untreated cells, the Fn/c values of STAT1 were similar for mock-, Nishigahara-, Ni-CE-, and CE(NiP)-infected cells (Fig. 4B). On the other hand, in IFN-α-treated cells, the Fn/c values for STAT1 in Ni-CE-infected cells were significantly greater than those in Nishigahara- or CE(NiP)-infected cells ($P < 0.0001$). These data strongly suggest that the P protein is responsible for the different inhibitory effects of Nishigahara and Ni-CE infections on IFN-induced STAT1 nuclear translocation.

Ni-CE P protein is defective in its capacity to inhibit STAT1 nuclear translocation. Next, we examined whether single expression of Nishigahara P protein but not Ni-CE P protein is sufficient to block the nuclear translocation of IFN-activated STAT1. We transfected Vero cells to express Nishigahara or Ni-CE P protein fused to GFP (Ni P-GFP and Ni-CE P-GFP, respectively) and treated the cells with or without IFN-α before fixation, immunostaining for STAT1, and CLSM analysis. In the IFN-α-untreated cells, STAT1 was more cytoplasmic than nuclear (Fig. 5A, top, and B) and the localization did not differ significantly between Ni P-GFP- and Ni-CE P-GFP-expressing cells (Fig. 5B). In contrast, in IFN-α-treated cells, STAT1 localization differed significantly between cells express-

ing Ni P-GFP and Ni-CE P-GFP (Fig. 5A, bottom, and B). Specifically, STAT1 was retained in the cytoplasm in Ni P-GFP-expressing cells, consistent with previous observations for P proteins from other RV strains (4, 36). On the other hand, STAT1 in Ni-CE P-GFP-expressing cells was able to translocate to and accumulate within the nucleus such that the Fn/c of STAT1 in IFN-α-treated, Ni-CE P-GFP-expressing cells was approximately 7-fold higher than in equivalently treated cells expressing Ni P-GFP ($P < 0.0001$) (Fig. 5B). Similar results were obtained from transfected Vero cells treated with IFN-γ and transfected SK-N-SH cells treated with IFN-α or IFN-γ (data not shown).

Taken together with the data from virus-infected cells (Fig. 4), these data demonstrate that Nishigahara P protein is able to block the nuclear translocation of IFN-activated STAT1 more efficiently than Ni-CE P protein and indicate that the inhibitory effect of RV P protein on STAT1 translocation correlates with viral pathogenicity.

Nishigahara and Ni-CE P proteins show differing subcellular localization. Sequence analysis indicated that the previously identified CRM1-dependent nuclear export signal (NES) (conforming to the motif LXXXLXXLXL, where L can be replaced with M, I, V, or F), which is principally responsible for nuclear exclusion of the P protein of the RV CVS-11 strain (20), is conserved in the Nishigahara P protein (49 LPEDMS RLHL 58; the motif is indicated in boldface) but not in the Ni-CE P protein, due to two amino acid substitutions (49 LPEDMSRPHP 58; substitutions are underlined) (Fig. 1B) (30). To check whether the amino acid substitutions in the Ni-CE P protein affect its subcellular localization, we compared the distribution of Ni P-GFP and Ni-CE P-GFP in transfected Vero (Fig. 5A) and SK-N-SH cells (not shown). We found that Ni P-GFP was localized in the cytoplasm (Fig. 5A, top) and was almost completely excluded from the nucleus (Fn/c, 0.22 ± 0.13) (Fig. 5C). In contrast, Ni-CE P-GFP was localized more diffusely between the nucleus and cytoplasm, resulting in 4-fold greater levels of accumulation in the nucleus (Fn/c: 0.87 ± 0.32) ($P < 0.0001$) (Fig. 5A, top, and C) than for Ni P-GFP. Interestingly, Ni-CE P-GFP was found to become significantly more nuclear after IFN-α treatment ($P < 0.0001$) (Fig. 5A, bottom, and C). In contrast, the nucleocytoplasmic localization of Ni P-GFP was unaffected by IFN-α treatment.

We also examined the nucleocytoplasmic distribution of Ni-CE P protein and Nishigahara P protein in RV-infected SK-N-SH cells by fixation and immunostaining for P protein. Nishigahara P protein was localized almost exclusively in the cytoplasm of Nishigahara- and CE(NiP)-infected cells (Fig. 6A and B), whereas Ni-CE P protein was more diffusely localized between the nucleus and cytoplasm ($P < 0.0001$). There was no obvious fluorescent signal in mock-infected cells (Fig. 6A), confirming that the signals detected in infected cells were specific for the P protein. These results indicate that the Ni-CE P protein is defective in nuclear export due to the mutagenic inactivation of the NES and strongly suggest that this results in inhibition of the capacity of Ni-CE P protein to regulate STAT1 nuclear import.

Both Nishigahara and Ni-CE P protein can interact with STAT1. Sequence analysis showed that the previously identified STAT1-binding domain (36) is conserved between the Nishigahara and Ni-CE P proteins (Fig. 1B). This predicts that both P proteins should maintain the ability to bind to STAT1. To confirm the physical interaction between the Nishigahara and Ni-CE P proteins and STAT1, we used the yeast two-hybrid system. The yeast L40 strain that contains the two LexA-responsive reporter genes LacZ and His3 was cotransformed with the pLexA-Ni P or -Ni-CE P plasmid, which encode BD-fused Nishigahara and Ni-CE P proteins, respec-

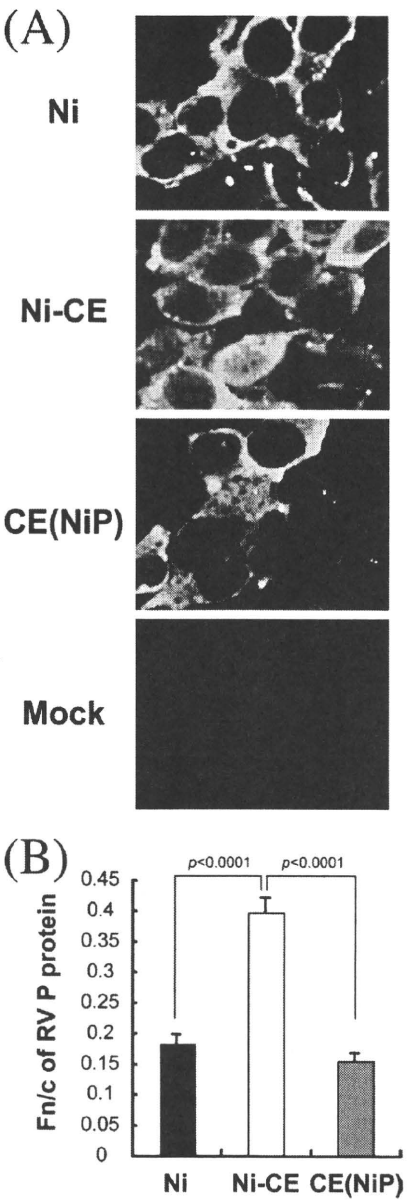

FIG. 6. The Nishigahara (Ni) and Ni-CE P proteins show differing subcellular localizations in infected SK-N-SH cells. (A) The cells were inoculated with each strain at an MOI of 0.01 and, after 24 h, were fixed with 3.7% formaldehyde for 10 min and 90% methanol for 5 min. The fixed cells were subjected to immunostaining for RV P protein and analyzed by CLSM. Dot structures observed in the cytoplasm represent Negri bodies (12). (B) Images such as those shown in panel A were used to calculate the ratio of nuclear to cytoplasmic fluorescence (Fn/c) values, which are shown as the means ± standard errors of the means of the results from >30 images.

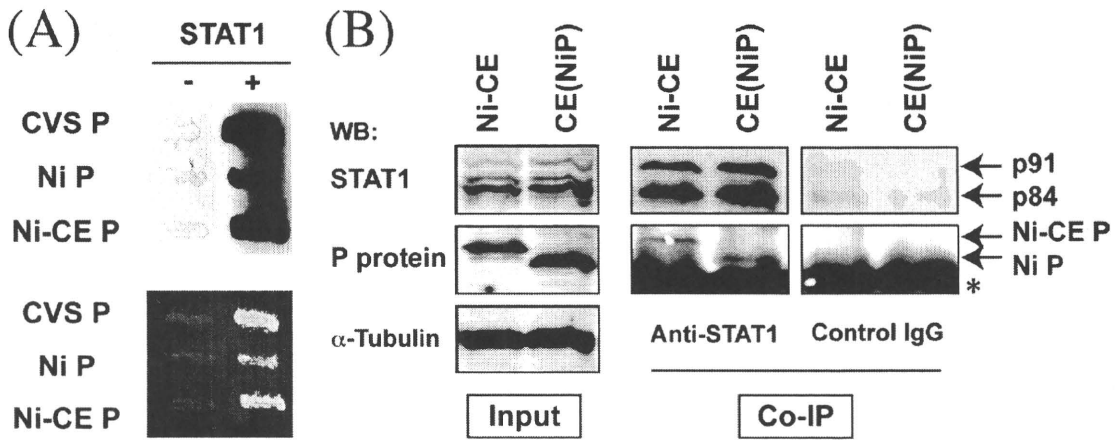

FIG. 7. Both the Nishigahara (Ni) and Ni-CE P proteins physically interact with STAT1. (A) Yeast cells (L40 strain) were cotransformed with plasmid pLex-CVS P, -Ni P, or -Ni-CE P and plasmid pGAD-STAT1 (+) or the empty pGAD plasmid (−). The P protein-STAT1 interaction was assessed by the appearance of blue colonies in the presence of X-Gal on a plate lacking Trp and Leu (upper panel) and by the expression of the His3 reporter gene on a plate lacking Trp, Leu, and His (lower panel). (B) SK-N-SH cells were inoculated with strain Ni-CE or CE(NiP) at an MOI of 0.1. At 18 h p.i., the cells were treated with IFN-α for 2 h before being lysed in RIPA buffer. The cell lysates were subjected to co-IP analysis with an anti-STAT1 antibody or control rabbit IgG. The precipitates and total lysate (input) were analyzed by Western blotting (WB). The asterisk represents an additional band probably resulting from binding of antibodies used for Western blotting to protein A/G. α-Tubulin, alpha-tubulin.

tively, and pGAD-STAT1 expressing AD-fused STAT1. In addition, we used a combination of pLexA-CVS P, which expresses BD-fused P protein of RV strain CVS, and pGAD-STAT1 as a positive control (36). We found that BD-fused P proteins derived from each of the CVS, Nishigahara, and Ni-CE strains, when coexpressed with AD-fused STAT1, were able to activate transcription of LacZ to comparable extents (Fig. 7A, top) and could also activate His3 gene expression, resulting in comparable growth on a plate lacking Trp, Leu, and His (Fig. 7A, bottom). These data demonstrate that both Nishigahara and Ni-CE P protein physically interact with STAT1.

Next, to check the interaction of the Nishigahara and Ni-CE P proteins with STAT1 in infected cells, we carried out co-IP analysis (Fig. 7B). Lysates of SK-N-SH cells infected with strain Ni-CE or CE(NiP) were subjected to IP with an anti-STAT1 antibody or control rabbit IgG. We found that both Ni-CE and Nishigahara P protein were detected in the precipitates after IP with an anti-STAT1 antibody (Fig. 7B, middle) but not after IP with control IgG (Fig. 7B, right). The amounts of Ni-CE and Nishigahara P proteins detected in the precipitates were comparable, indicating that the interactions of Ni-CE and Nishigahara P proteins with STAT1 occur with similar efficiencies.

The NES in RV P protein is important for IFN antagonism. Despite the fact that the Ni-CE P protein maintains the ability to bind to STAT1, the P protein cannot block nuclear translocation of IFN-activated STAT1. Taken together with the data above showing that the Ni-CE P protein is diffusely localized between the nucleus and cytoplasm, probably due to the inactivation of NES, this strongly suggests that the NES in RV P protein is responsible for retention of the P protein-STAT1 complex in the cytoplasm to inhibit STAT1 nuclear translocation and, thereby, IFN signaling. To test this directly, we mutated the Ni-CE P-GFP to reinstate the functional NES by converting the Pro at positions 56 and 58 to Leu, producing Ni-CE P(NES$^+$)-GFP (Fig. 8A). We examined the subcellular localization of Ni-CE P(NES$^+$)-GFP, as well as its ability to inhibit STAT1 nuclear translocation. In contrast to Ni-CE P-GFP, Ni-CE P(NES$^+$)-GFP was distributed mainly in the cytoplasm in live SK-N-SH cells (Fig. 8B). Also, we found that Ni-CE P(NES$^+$)-GFP was significantly more cytoplasmic than Ni-CE P-GFP in Vero cells both treated and untreated with IFN-α ($P < 0.0001$) (Fig. 8C and D). Importantly, nuclear translocation of IFN-activated STAT1 was inhibited in Vero cells expressing Ni-CE P(NES$^+$)-GFP but not in Vero cells expressing Ni-CE P-GFP (Fig. 8C and E).

Next, we compared IFN-α-induced ISRE activities in SK-N-SH cells transfected to express Ni P-GFP, Ni-CE P-GFP, or Ni-CE P(NES$^+$)-GFP (Fig. 8F). We found that the expression of Ni-CE P(NES$^+$)-GFP suppressed ISRE activity more efficiently than Ni-CE P-GFP ($P < 0.01$). Notably, there was no statistically significant difference between the activities in Ni P-GFP- and Ni-CE P(NES$^+$)-GFP-expressing cells. These results indicate that the NES on the RV P protein plays an important role in the inhibition of STAT1 nuclear translocation and, thereby, of IFN signaling.

DISCUSSION

RV is a neurotropic virus that causes encephalomyelitis with a high mortality rate (almost 100%) in humans and other mammals, for which no effective cure has been established, resulting in approximately 55,000 human fatalities in Asia and Africa per annum (11). To develop an effective cure, it is important to fully understand the molecular mechanism by which RV circumvents host immune response and, consequently, causes the lethal neurological disease. To date, RV glycoprotein (G protein), which participates in binding to host cells, has been shown to play important roles in the viral pathogenicity (7, 10, 27, 32–35), but little is known about the contribution of other RV proteins to pathogenicity.

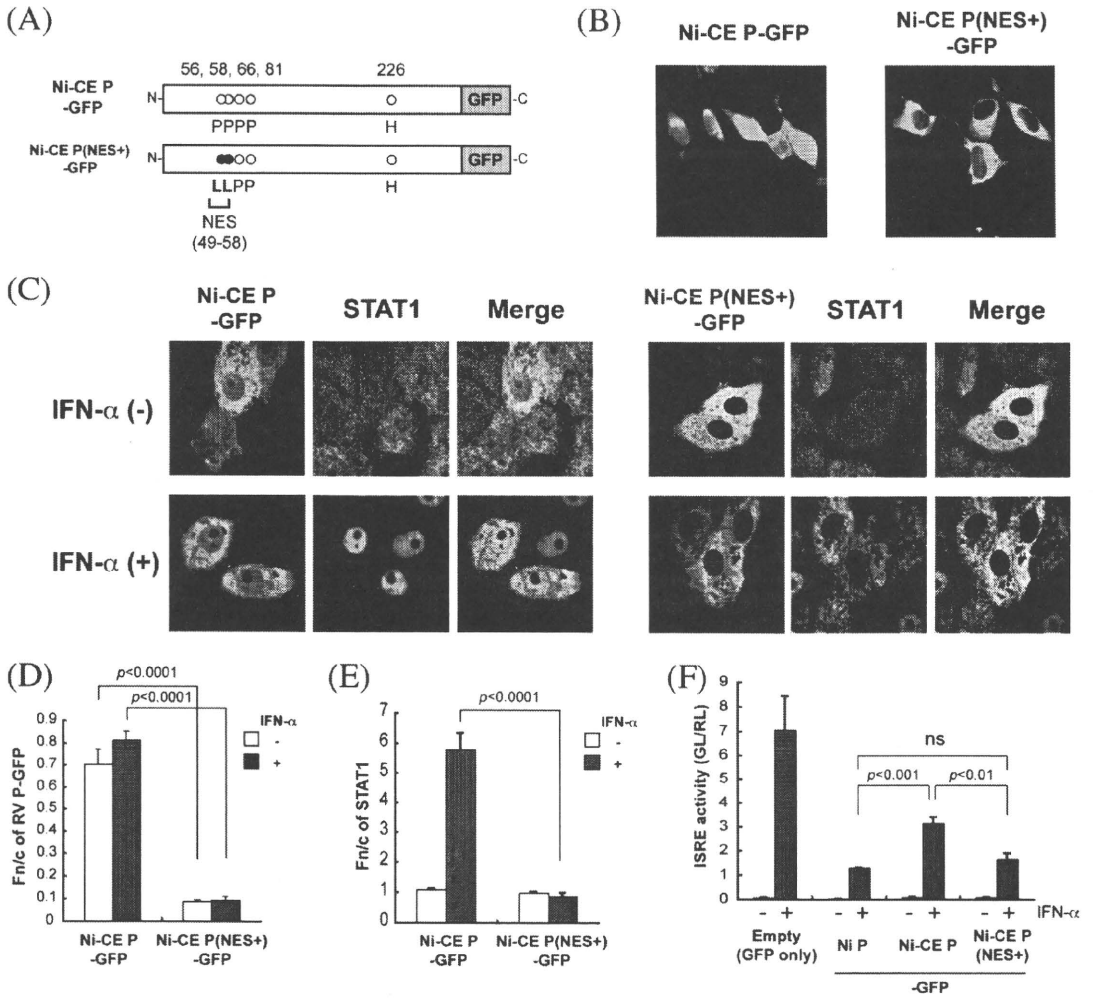

FIG. 8. The NES in RV P protein plays an important role in its IFN antagonism. (A) In order to restore the NES activity to the Ni-CE P protein [producing Ni-CE P(NES$^+$)-GFP], Pro-to-Leu substitutions were introduced into Ni-CE P-GFP at positions 56 and 58. (B) To compare the subcellular localization of Ni-CE P(NES$^+$)-GFP with that of Ni-CE P-GFP, SK-N-SH cells were transfected with plasmid pEGFP-N1 expressing the respective protein and images were collected 24 h posttransfection. (C) Vero cells were transfected to express Ni-CE P-GFP or Ni-CE P(NES$^+$)-GFP (green) and treated with or without IFN-α before being fixed and immunostained for STAT1 (red) and analyzed by CLSM. (D, E) Images such as those shown in panel C were analyzed to derive the ratio of nuclear to cytoplasmic fluorescence (Fn/c) values (mean ± standard error of the mean, $n > 30$) for GFP-tagged P protein (D) or STAT1 (E). (F) SK-N-SH cells were transfected with the ISRE reporter and the control plasmids, together with the pEGFP-N1 plasmid expressing Ni-GFP, Ni-CE GFP, or Ni-CE P(NES$^+$)-GFP. At 24 h posttransfection, the cells were treated with IFN-α (2,000 U/ml) for 6 h and the cell lysates were subjected to the dual luciferase assay. GL, firefly luciferase activity; RL, *Renilla* luciferase activity; ns, not significant ($P \geq 0.05$).

The RV P protein can inhibit IFN signaling by physically interacting with STAT1, which has been hypothesized to relate to inhibition of STAT1 nuclear localization (4, 36). Thus, it has been assumed that these "IFN antagonist" proteins enable viruses to evade the innate immune system and thereby contribute to the viral pathogenicity. However, the importance of these mechanisms in viral pathogenicity remains unclear. Here, using both RV-infected cells and cells transfected to express only the RV P protein, we show for the first time that the capacity of the RV P protein to inhibit type I IFN signaling correlates with viral pathogenicity.

We found that the CE(NiP) strain grows more efficiently in the mouse brain than does the Ni-CE strain at the early stage of infection (3 days p.i.) (Fig. 1C). One possible explanation for this difference is that the P protein from the virulent Nishigahara strain functions to efficiently evade innate immunity, whereas the P protein from the attenuated Ni-CE strain is impaired in this function. In the present study, we tested this hypothesis, demonstrating that Nishigahara P protein inhibits type I IFN-activated STAT1 nuclear translocation and IFN signaling more efficiently than does Ni-CE P protein. Therefore, the difference in this P protein function appears to be directly related to the different pathogenicities of the two strains.

Brzózka et al. (3) demonstrated that the RV P protein also inhibits type I IFN induction by interfering with the phosphorylation of the transcription factor interferon regulatory factor 3 (IRF-3) by TANK-binding kinase 1. We found that infection of

human neuroblastoma SYM-I cells (9) with either the Ni-CE or CE(NiP) strain induces equivalent levels of IFN-β gene transcription (data not shown). Further, single expression of the Nishigahara and Ni-CE P proteins in SYM-I cells was equally inhibitory for the activation of the IRF-3-dependent IFN-β promoter induced by infection with Newcastle disease virus (13). These findings strongly suggest that the different pathogenicities of strains Nishigahara and Ni-CE do not relate to inhibition of IFN induction.

As the inhibition of IFN-activated STAT1 nuclear accumulation by P protein depends on the association of these molecules (4, 36), one possible explanation for the differences between the Nishigahara and Ni-CE P proteins was that the Ni-CE P protein might be unable to interact with STAT1. However, sequence analysis demonstrated that the C-terminal region within amino acid positions 267 to 297, previously identified as the STAT1-binding domain (36), is perfectly conserved between the Nishigahara and Ni-CE P proteins (Fig. 1B) (30). Importantly, the results of our yeast two-hybrid and co-IP analyses confirmed that both the Nishigahara and Ni-CE P proteins bind effectively to STAT1 (Fig. 7). Therefore, it appears that the different effects of the Nishigahara and Ni-CE P proteins on IFN signaling do not involve any significant differences in the capacity to interact with STAT1.

The P protein from the RV CVS strain is a nucleocytoplasmic shuttling protein with three distinct signals for nuclear transport: two NESs, corresponding to amino acids 49 to 58 (20) and 227 to 232 (16) and proximal to the N and C terminus, respectively, and a nuclear localization signal (NLS), including residues 211 to 214 and 260 (20). The NESs conform to a motif recognized by the nuclear export transport molecule CRM1, characterized by the presence of several hydrophobic residues (LXXXLXXLXL, where L can be replaced with M, I, V, or F). At steady state, the full-length P protein is almost entirely cytoplasmic, because the N-terminal NES constitutes the predominant signal (16, 20), but following treatment with leptomycin B (LMB), a specific inhibitor of CRM1-mediated nuclear export, RV P protein is able to accumulate in the nucleus because of the presence of the NLS (20). Importantly, the N-terminal NES (49 LPEDMSRLHL 58; the motif is indicated in bold) and C-terminal NLS (211 KKYK 214 and 260 R) are absolutely conserved in Nishigahara P protein. In contrast, the NES motif is destroyed in the Ni-CE P protein, because of amino acid substitutions at positions 56 and 58 (49 LPEDMS RPHP 58; the substitutions are underlined), while the C-terminal NLS is perfectly conserved (Fig. 1B). That these mutations efficiently inactivate the NES is indicated by the fact that Ni-CE P protein is able to localize in the nucleus and cytoplasm, whereas Nishigahara P protein is almost entirely excluded from the nucleus. Importantly, this difference was observed in both transfected (Fig. 5A and C) and infected cells (Fig. 6), providing the first evidence that the P protein can undergo nucleocytoplasmic trafficking in RV-infected cells, with significance for viral pathogenicity.

Interestingly, we also observed that Ni-CE P-GFP became significantly more nuclear after IFN-α treatment (Fig. 5A and C), suggesting that Ni-CE P protein is "piggybacked" into the nucleus due to the active nuclear import of the associated IFN-activated STAT1. In contrast, in Nishigahara P protein-expressing cells, nether STAT1 nor Ni P-GFP showed any enhancement of nuclear accumulation following IFN-α treatment (Fig. 5A and C). This strongly suggests that the P protein-STAT1 complex is excluded from the nucleus by the active nuclear export of the Nishigahara P protein component via its N-terminal NES. Consistent with this, we demonstrated that reconstitution of NES in Ni-CE P protein conferred the ability to inhibit IFN-activated STAT1 nuclear translocation (Fig. 8C and E) and, consequently, to suppress IFN-α-induced ISRE activity (Fig. 8F). These findings highlight the importance of the N-terminal NES in the IFN antagonist activity of RV P protein. A previous report using transfected cells showed that the capacity of P protein to block STAT1 nuclear accumulation was disabled by global inhibition of nuclear export by LMB treatment and that a truncated form of P protein (P3) that is actively localized to the nucleus (20) does not block the nuclear accumulation of STAT1 (37). The present report is the first to show that mutations within the N-terminal NES can disable nuclear export of P protein specifically, both in transfected and infected cells, as well as disabling its capacity to block STAT1 nuclear accumulation in these systems.

Despite the observations described above, Ni-CE P protein still modestly suppressed IFN-α-induced ISRE activity (Fig. 3A and B). Vidy et al. (37) previously reported that intranuclear RV P protein can inhibit the interaction of the STAT1-containining transcription factor complex ISGF3 with ISRE-containing DNA, to inhibit transcriptional activation. This function of the nuclear fraction of Ni-CE P protein (Fig. 5A and 6) might account for the residual activity observed.

Although RNA viruses have no clear requirement to interact with the cell nucleus, as their basic life cycle occurs entirely in the cytoplasm, it is interesting to note that many proteins encoded by RNA viruses are known to traffic into and/or out of the nucleus (1, 2, 5, 8, 15, 19, 21, 23, 28, 29), indicating that trafficking of these proteins is important to viral infection by permitting the virus to modulate nuclear processes, such as gene transcription. The present study provides fundamental information regarding the mechanism by which RV P protein determines viral pathogenicity, including evidence that the nucleocytoplasmic shuttling of RV P protein that causes retention of IFN-activated STAT1 in the cytoplasm correlates with viral pathogenicity. Also, our data identify a clear example showing the importance of IFN antagonism in viral pathogenicity, with significance for numerous medically important viruses and for the development of novel therapeutic approaches.

ACKNOWLEDGMENTS

We thank Akihiko Kawai (Research Institute for Production and Development, Japan) for providing an anti-RV P protein rabbit serum. We are grateful to Jacques Camonis (Institut Curie, France) for the plasmids pLexA and pGAD. We acknowledge Cassandra David for assistance with tissue culture, and we express our appreciation for the facilities and technical assistance of Monash Micro Imaging, Monash University, Victoria, Australia.

This study was partially supported by a grant (project code no. I-AD14-2009-11-01) from the National Veterinary Research and Quarantine Service, Ministry for Food, Agriculture, Forestry, and Fisheries, South Korea, in 2008, and by NHMRC project grant no. 535838.

REFERENCES

1. **Billecocq, A., M. Spiegel, P. Vialat, A. Kohl, F. Weber, M. Bouloy, and O. Haller.** 2004. NSs protein of Rift Valley fever virus blocks interferon production by inhibiting host gene transcription. J. Virol. **78**:9798–9806.
2. **Breakwell, L., P. Dosenovic, G. B. Karlsson Hedestam, M. D'Amato, P. Liljestrom, J. Fazakerley, and G. M. McInerney.** 2007. Semliki Forest virus nonstructural protein 2 is involved in suppression of the type I interferon response. J. Virol. **81**:8677–8684.
3. **Brzózka, K., S. Finke, and K. K. Conzelmann.** 2005. Identification of the rabies virus alpha/beta interferon antagonist: phosphoprotein P interferes with phosphorylation of interferon regulatory factor 3. J. Virol. **79**:7673–7681.
4. **Brzózka, K., S. Finke, and K. K. Conzelmann.** 2006. Inhibition of interferon signaling by rabies virus phosphoprotein P: activation-dependent binding of STAT1 and STAT2. J. Virol. **80**:2675–2683.
5. **Chelbi-Alix, M. K., A. Vidy, J. El Bougrini, and D. Blondel.** 2006. Rabies viral mechanisms to escape the IFN system: the viral protein P interferes with IRF-3, Stat1, and PML nuclear bodies. J. Interferon Cytokine Res. **26**:271–280.
6. **Delhaye, S., S. Paul, G. Blakqori, M. Minet, F. Weber, P. Staeheli, and T. Michiels.** 2006. Neurons produce type I interferon during viral encephalitis. Proc. Natl. Acad. Sci. U. S. A. **103**:7835–7840.
7. **Dietzschold, B., W. H. Wunner, T. J. Wiktor, A. D. Lopes, M. Lafon, C. L. Smith, and H. Koprowski.** 1983. Characterization of an antigenic determinant of the glycoprotein that correlates with pathogenicity of rabies virus. Proc. Natl. Acad. Sci. U. S. A. **80**:70–74.
8. **Ghildyal, R., A. Ho, M. Dias, L. Soegiyono, P. G. Bardin, K. C. Tran, M. N. Teng, and D. A. Jans.** 2009. The respiratory syncytial virus matrix protein possesses a Crm1-mediated nuclear export mechanism. J. Virol. **83**:5353–5362.
9. **Honda, Y., A. Kawai, and S. Matsumoto.** 1984. Comparative studies of rabies and Sindbis virus replication in human neuroblastoma (SYM-I) cells that can produce interferon. J. Gen. Virol. **65**(Pt. 10):1645–1653.
10. **Ito, N., M. Takayama, K. Yamada, M. Sugiyama, and N. Minamoto.** 2001. Rescue of rabies virus from cloned cDNA and identification of the pathogenicity-related gene: glycoprotein gene is associated with virulence for adult mice. J. Virol. **75**:9121–9128.
11. **Knobel, D. L., S. Cleaveland, P. G. Coleman, E. M. Fevre, M. I. Meltzer, M. E. Miranda, A. Shaw, J. Zinsstag, and F. X. Meslin.** 2005. Re-evaluating the burden of rabies in Africa and Asia. Bull. World Health Organ. **83**:360–368.
12. **Lahaye, X., A. Vidy, C. Pomier, L. Obiang, F. Harper, Y. Gaudin, and D. Blondel.** 2009. Functional characterization of Negri bodies (NBs) in rabies virus-infected cells: evidence that NBs are sites of viral transcription and replication. J. Virol. **83**:7948–7958.
13. **Masatani, T., N. Ito, K. Shimizu, Y. Ito, K. Nakagawa, Y. Sawaki, H. Koyama, and M. Sugiyama.** 2010. Rabies virus nucleoprotein functions to evade activation of RIG-I-mediated antiviral response. J. Virol. **84**:4002–4012.
14. **Minamoto, N., H. Tanaka, M. Hishida, H. Goto, H. Ito, S. Naruse, K. Yamamoto, M. Sugiyama, T. Kinjo, K. Mannen, and K. Mifune.** 1994. Linear and conformation-dependent antigenic sites on the nucleoprotein of rabies virus. Microbiol. Immunol. **38**:449–455.
15. **Montgomery, S. A., and R. E. Johnston.** 2007. Nuclear import and export of Venezuelan equine encephalitis virus nonstructural protein 2. J. Virol. **81**: 10268–10279.
16. **Moseley, G. W., R. P. Filmer, M. A. DeJesus, and D. A. Jans.** 2007. Nucleocytoplasmic distribution of rabies virus P-protein is regulated by phosphorylation adjacent to C-terminal nuclear import and export signals. Biochemistry **46**:12053–12061.
17. **Moseley, G. W., X. Lahaye, D. M. Roth, S. Oksayan, R. P. Filmer, C. L. Rowe, D. Blondel, and D. A. Jans.** 2009. Dual modes of rabies P-protein association with microtubules: a novel strategy to suppress the antiviral response. J. Cell Sci. **122**(Pt. 20):3652–3662.
18. **Moseley, G. W., D. M. Roth, M. A. DeJesus, D. L. Leyton, R. P. Filmer, C. W. Pouton, and D. A. Jans.** 2007. Dynein light chain association sequences can facilitate nuclear protein import. Mol. Biol. Cell **18**:3204–3213.
19. **Nishie, T., K. Nagata, and K. Takeuchi.** 2007. The C protein of wild-type measles virus has the ability to shuttle between the nucleus and the cytoplasm. Microbes Infect. **9**:344–354.
20. **Pasdeloup, D., N. Poisson, H. Raux, Y. Gaudin, R. W. Ruigrok, and D. Blondel.** 2005. Nucleocytoplasmic shuttling of the rabies virus P protein requires a nuclear localization signal and a CRM1-dependent nuclear export signal. Virology **334**:284–293.
21. **Pryor, M. J., S. M. Rawlinson, R. E. Butcher, C. L. Barton, T. A. Waterhouse, S. G. Vasudevan, P. G. Bardin, P. J. Wright, D. A. Jans, and A. D. Davidson.** 2007. Nuclear localization of dengue virus nonstructural protein 5 through its importin alpha/beta-recognized nuclear localization sequences is integral to viral infection. Traffic **8**:795–807.
22. **Randall, R. E., and S. Goodbourn.** 2008. Interferons and viruses: an interplay between induction, signalling, antiviral responses and virus countermeasures. J. Gen. Virol. **89**:1–47.
23. **Rawlinson, S. M., M. J. Pryor, P. J. Wright, and D. A. Jans.** 2009. CRM1-mediated nuclear export of dengue virus RNA polymerase NS5 modulates interleukin-8 induction and virus production. J. Biol. Chem. **284**:15589–15597.
24. **Reid, S. P., L. W. Leung, A. L. Hartman, O. Martinez, M. L. Shaw, C. Carbonnelle, V. E. Volchkov, S. T. Nichol, and C. F. Basler.** 2006. Ebola virus VP24 binds karyopherin alpha1 and blocks STAT1 nuclear accumulation. J. Virol. **80**:5156–5167.
25. **Rodriguez, J. J., J. P. Parisien, and C. M. Horvath.** 2002. Nipah virus V protein evades alpha and gamma interferons by preventing STAT1 and STAT2 activation and nuclear accumulation. J. Virol. **76**:11476–11483.
26. **Roth, D. M., G. W. Moseley, D. Glover, C. W. Pouton, and D. A. Jans.** 2007. A microtubule-facilitated nuclear import pathway for cancer regulatory proteins. Traffic **8**:673–686.
27. **Seif, I., P. Coulon, P. E. Rollin, and A. Flamand.** 1985. Rabies virulence: effect on pathogenicity and sequence characterization of rabies virus mutations affecting antigenic site III of the glycoprotein. J. Virol. **53**:926–934.
28. **Shaw, M. L., W. B. Cardenas, D. Zamarin, P. Palese, and C. F. Basler.** 2005. Nuclear localization of the Nipah virus W protein allows for inhibition of both virus- and toll-like receptor 3-triggered signaling pathways. J. Virol. **79**:6078–6088.
29. **Shaw, M. L., A. Garcia-Sastre, P. Palese, and C. F. Basler.** 2004. Nipah virus V and W proteins have a common STAT1-binding domain yet inhibit STAT1 activation from the cytoplasmic and nuclear compartments, respectively. J. Virol. **78**:5633–5641.
30. **Shimizu, K., N. Ito, T. Mita, K. Yamada, J. Hosokawa-Muto, M. Sugiyama, and N. Minamoto.** 2007. Involvement of nucleoprotein, phosphoprotein, and matrix protein genes of rabies virus in virulence for adult mice. Virus Res. **123**:154–160.
31. **Shimizu, K., N. Ito, M. Sugiyama, and N. Minamoto.** 2006. Sensitivity of rabies virus to type I interferon is determined by the phosphoprotein gene. Microbiol. Immunol. **50**:975–978.
32. **Takayama-Ito, M., K. Inoue, Y. Shoji, S. Inoue, T. Iijima, T. Sakai, I. Kurane, and K. Morimoto.** 2006. A highly attenuated rabies virus HEP-Flury strain reverts to virulent by single amino acid substitution to arginine at position 333 in glycoprotein. Virus Res. **119**:208–215.
33. **Takayama-Ito, M., N. Ito, K. Yamada, N. Minamoto, and M. Sugiyama.** 2004. Region at amino acids 164 to 303 of the rabies virus glycoprotein plays an important role in pathogenicity for adult mice. J. Neurovirol. **10**:131–135.
34. **Takayama-Ito, M., N. Ito, K. Yamada, M. Sugiyama, and N. Minamoto.** 2006. Multiple amino acids in the glycoprotein of rabies virus are responsible for pathogenicity in adult mice. Virus Res. **115**:169–175.
35. **Tuffereau, C., H. Leblois, J. Benejean, P. Coulon, F. Lafay, and A. Flamand.** 1989. Arginine or lysine in position 333 of ERA and CVS glycoprotein is necessary for rabies virulence in adult mice. Virology **172**:206–212.
36. **Vidy, A., M. Chelbi-Alix, and D. Blondel.** 2005. Rabies virus P protein interacts with STAT1 and inhibits interferon signal transduction pathways. J. Virol. **79**:14411–14420.
37. **Vidy, A., J. El Bougrini, M. K. Chelbi-Alix, and D. Blondel.** 2007. The nucleocytoplasmic rabies virus P protein counteracts interferon signaling by inhibiting both nuclear accumulation and DNA binding of STAT1. J. Virol. **81**:4255–4263.
38. **Yamada, K., N. Ito, M. Takayama-Ito, M. Sugiyama, and N. Minamoto.** 2006. Multigenic relation to the attenuation of rabies virus. Microbiol. Immunol. **50**:25–32.

Virus Research 155 (2011) 168–174

Contents lists available at ScienceDirect

Virus Research

journal homepage: www.elsevier.com/locate/virusres

Amino acids at positions 273 and 394 in rabies virus nucleoprotein are important for both evasion of host RIG-I-mediated antiviral response and pathogenicity

Tatsunori Masatani[a], Naoto Ito[a,b], Kenta Shimizu[a,1], Yuki Ito[a], Keisuke Nakagawa[a], Masako Abe[a], Satoko Yamaoka[a], Makoto Sugiyama[a,b,*]

[a] The United Graduate School of Veterinary Sciences, Gifu University, 1-1 Yanagido, Gifu 501-1193, Japan
[b] Laboratory of Zoonotic Diseases, Faculty of Applied Biological Sciences, Gifu University, 1-1 Yanagido, Gifu 501-1193, Japan

ARTICLE INFO

Article history:
Received 5 July 2010
Received in revised form 3 September 2010
Accepted 19 September 2010
Available online 25 September 2010

Keywords:
Rabies virus
Nucleoprotein
Pathogenicity
Innate immunity
Retinoic acid-inducible gene I

ABSTRACT

We previously reported that nucleoprotein (N) is related to the different pathogenicities of the virulent rabies virus strain Nishigahara (Ni) and avirulent strain Ni-CE and also that Ni N, but not Ni-CE N, functions to evade retinoic acid-inducible gene I (RIG-I)-mediated innate immunity. There are three amino acid differences between Ni and Ni-CE N (at positions 273, 394 and 395), indicating that one of these mutations or a combination of mutations is important for the pathogenicity and evasion of innate immunity. We generated Ni-CE mutants in which the amino acids in Ni-CE N were replaced with those of Ni in all combinations. Among the mutants, CE(NiN273/394) with mutations at positions 273 and 394 evaded activation of RIG-I-mediated signaling most efficiently and also showed the highest pathogenicity. This correlation reinforces the relation between evasion of host RIG-I-mediated innate immunity and pathogenicity of rabies virus.

1. Introduction

Rabies is a fatal neurological disease that affects almost all kinds of mammals, including humans. The etiological agent, rabies virus, belongs to *Lyssavirus* of the family *Rhabdoviridae*. The genome is an unsegmented negative-sense RNA and contains five genes (N, P, M, G and L genes) encoding nucleoprotein (N protein), phosphoprotein (P protein), matrix (M) protein, glycoprotein (G protein) and large (L) protein, respectively. N, P and L proteins constitute a ribonucleoprotein (RNP) complex together with viral genomic RNA (Finke and Conzelmann, 2005; Schnell et al., 2010). The N protein enwraps viral RNA to form a functional template for transcription and replication. The L protein functions as an RNA-dependent RNA polymerase together with the P protein, which is known as a cofactor of the polymerase. During virus assembly, the RNP complex is wrapped into an envelope containing the M and G proteins (Finke and Conzelmann, 2003; Mebatsion et al., 1999).

The host innate immune response is the first defense line to prevent viral infection. A key aspect of the antiviral innate immune response is the synthesis and secretion of type I interferons (IFN) such as IFN-α and -β, which induce an antiviral status of cells (Haller et al., 2006; Randall and Goodbourn, 2008). The antiviral innate immune response is triggered when viral infection is recognized by specific cellular pathogen recognition receptors (Akira et al., 2006). It has been reported that infections with negative-stranded RNA viruses including rabies virus are recognized by a cellular sensor protein, retinoic acid-inducible gene I (RIG-I) (Hornung et al., 2006; Rehwinkel and Reis e Sousa, 2010; Yoneyama et al., 2004). After recognition of viral infection, RIG-I triggers activation of a transcription factor, interferon regulatory factor-3 (IRF-3), and consequently induction of type I IFN and some chemokines, which are important for host innate immunity and inflammation, respectively (Genin et al., 2000; Honda and Taniguchi, 2006; Lefort et al., 2007; Nakaya et al., 2001). Previously, it was shown that neurons in the brain produce type I IFN and are also capable of responding to the produced type I IFN (Daffis et al., 2007; Delhaye et al., 2006). The fact that rabies virus can efficiently replicate in brain neurons strongly suggests that the virus has a certain mechanism to circumvent host innate immunity. However, the

Abbreviations: RIG-I, retinoic acid-inducible gene I; N protein, nucleoprotein; P protein, phosphoprotein; M protein, matrix protein; G protein, glycoprotein; L protein, large protein; RNP, ribonucleoprotein; IFN, interferon; IRF-3, interferon regulatory factor-3; Ni, Nishigahara; i.c., intracerebral; E-MEM, Eagle's minimum essential medium; FCS, fetal calf serum; RT, reverse transcription; MOI, multiplicity of infection; dpi, days post-infection; FFU, focus-forming units; hpi, hours post-infection; SD, standard deviation; GAPDH, glyceraldehyde 3-phosphate dehydrogenase; LD_{50}, 50% lethal dose; NTD, N-terminal core domain; CTD, C-terminal core domain; DI, defective-interference.

* Corresponding author at: Laboratory of Zoonotic Diseases, Faculty of Applied Biological Sciences, Gifu University, 1-1 Yanagido, Gifu 501-1193, Japan. Tel.: +81 58 293 2948; fax: +81 58 293 2948.
E-mail address: sugiyama@gifu-u.ac.jp (M. Sugiyama).
[1] Present address: Department of Microbiology, Graduate School of Medicine, Hokkaido University, Kita-15, Nishi-7, Kita-ku, Sapporo, Japan.

0168-1702/$ – see front matter © 2010 Elsevier B.V. All rights reserved.
doi:10.1016/j.virusres.2010.09.016

importance of evasion of host innate immunity in viral pathogenicity has not been elucidated.

The fixed rabies virus Nishigahara (Ni) strain kills adult mice after intracerebral (i.c.) inoculation, whereas Ni-CE strain, which was established after 100 passages of Ni strain in chicken embryo fibroblast cells, causes non-lethal infection in adult mice. We have demonstrated that a chimeric CE(NiN) strain, which has the N gene from Ni strain in the Ni-CE genome, killed adult mice after i.c. inoculation (Shimizu et al., 2007). This indicated that the N gene is related to the different pathogenicities of Ni and Ni-CE strains. Moreover, very recently, we reported that Ni N protein functions in evasion of host innate immunity (Masatani et al., 2010). We demonstrated that the expression levels of IFN-β and some chemokine genes in Ni- and CE(NiN)-infected human neuroblastoma cells were lower than the levels in Ni-CE-infected cells. We also showed that Ni N protein has a function to evade activation of RIG-I. These results strongly suggest that evasion of RIG-I-mediated host innate immunity by Ni N protein correlates with viral pathogenicity.

The fact that there are three amino acid differences in the N protein between Ni and Ni-CE strains (Phe to Leu at position 273 [indicated as a mutation from Ni strain to Ni-CE strain], Tyr to His at 394, and Phe to Leu at 395) indicates that one or a combination of these mutations is important for evasion of RIG-I-mediated host innate immunity and pathogenicity. In this study, to determine which amino acids in N protein are important for both phenotypes, we generated six Ni-CE mutants in which one or two amino acids in N protein were replaced with those from the Ni strain in the genomic backbone of the Ni-CE strain. Among the mutants, CE(NiN273/394) strain with mutations at positions 273 and 394 evaded activation of RIG-I-mediated signaling most efficiently and also showed the highest pathogenicity. This highlights the importance of evasion of RIG-I-mediated host innate immunity in viral pathogenicity.

2. Materials and methods

2.1. Cells and viruses

Human neuroblastoma SYM-I cells (kindly provided by Dr. A. Kawai) and mouse neuroblastoma NA cells were maintained in Eagle's minimum essential medium (E-MEM; Wako, Osaka, Japan) supplemented with 10% fetal calf serum (FCS). A baby hamster kidney BHK cell clone, BHK/T7-9 cells (Ito et al., 2003), which constitutively express T7 RNA polymerase, were maintained in E-MEM supplemented with 10% tryptose phosphate broth and 5% FCS. Recombinant Ni, Ni-CE and CE(NiN) strains were recovered from the cloned cDNA of the respective strains as reported previously (Shimizu et al., 2007). Stocks of all rabies virus strains were propagated in NA cells.

2.2. Generation of mutant rabies viruses

Full-genome plasmids for Ni-CE mutants, CE(NiN273), CE(NiN394), CE(NiN395), CE(NiN273/394), CE(NiN273/395) and CE(NiN394/395) strains, were constructed by using a QuickChange Site-Directed Mutagenesis Kit (Stratagene, La Jolla, CA). Detailed information of the construction of these plasmids is available from the authors on request. The mutant viruses were recovered from these genome plasmids using a reverse genetics system as reported previously (Ito et al., 2003; Yamada et al., 2006). Briefly, three helper plasmids (pT7IRES-RN, -RP and -RL) expressing rabies virus N, P and L under the control of T7 RNA polymerase were transfected into BHK/T7-9 cells together with the respective full-length genome plasmid using TransIT-LT1 reagent (Mirus Bio, Madison, WI, USA). After incubation for 4 days, viruses in culture supernatants were collected. The nucleotide sequence of each N gene was confirmed by direct sequencing with reverse transcription (RT)-PCR fragments from the final recombinant viruses.

2.3. Virus growth in NA cells

Monolayer cultures of NA cells were infected with each virus at a multiplicity of infection (MOI) of 0.01. At 3 days post-infection (dpi), titers of the rabies viruses in the supernatant of the cells were determined by an immunofluorescent antibody assay using monoclonal antibody 13–27 specific for N protein (Minamoto et al., 1994) and FITC-goat anti mouse IgG (Cappel, West Chester, PA, USA). Foci of infected cells were counted using Axiovert 200 (Carl Zeiss, Jena, Germany) and viral titers were calculated as focus-forming units (FFU) per milliliter.

2.4. Western blotting

Confluent SYM-I cells were inoculated with Ni, Ni-CE, CE(NiN) and Ni-CE mutants at an MOI of 2. At 24 h post-infection (hpi), cells were lysed and expression levels of N protein and α-tubulin were analyzed by Western blotting as described previously (Masatani et al., 2010).

2.5. Reporter assay

SYM-I cells were inoculated, in suspension, with Ni, Ni-CE and Ni-CE mutants at an MOI of 2 and seeded in a 24-well tissue culture plate (Greiner Bio-one, Frickenhausen, Germany) at 2×10^5 cells per well. At 24 hpi, cells were transfected with 1 μg of pEF-Flag-RIG-IC, pEF-Flag-RIG-IN or empty vector pEF-BOS(+) (each plasmid kindly provided by Dr. T. Fujita) (Yoneyama et al., 2004), in addition to 0.25 μg of 4× IRF3-Luc (kindly provided by Dr. S. Ludwig) which contains four copies of the IRF-3-binding PRD I/III motif of the IFN-β promoter upstream of the luciferase reporter gene (Ehrhardt et al., 2004), and 0.04 μg of pRL-TK (Promega, Madison, WI, USA) used as a control for transfection efficiency in the dual-luciferase reporter assay, which contains the *Renilla* luciferase gene downstream of the herpes simplex virus thymidine kinase promoter, using Lipofectamine 2000 (Invitrogen, Carlsbad, CA, USA) and incubated for 24 h. In another experiment, SYM-I cells were transfected with 1 μg of pEF-Flag-RIG-I (kindly provided by Dr. T. Fujita) or pEF-BOS(+), in addition to 0.25 μg of 4× IRF3-Luc and 0.04 μg of pRL-TK. At 24 h post-transfection, cells were infected with Ni, Ni-CE, CE(NiN) and Ni-CE mutants at an MOI of 2 and incubated for 24 h.

At the completion of the experiments, cells were lysed, and the activities of firefly and *Renilla* luciferases were determined by a Dual-Luciferase Reporter Assay System (Promega) according to the manufacturer's instructions. Data represent firefly luciferase activity normalized to *Renilla* luciferase activity. All assays were carried out in triplicate and the results are expressed as means ± standard deviation (SD).

2.6. Real-time RT-PCR

SYM-I cells grown in a 24-well tissue culture plate (Greiner Bio-one) were inoculated with each rabies virus strain at an MOI of 2 and incubated. At 24 hpi, total cellular RNA extraction and RT reaction were performed by using an RNeasy Mini Plus Total RNA extraction kit (QIAGEN, Valencia, CA, USA) and SuperScript III reverse transcriptase (Invitrogen) with oligo-$(dT)_{20}$, respectively. Real-time PCR reaction was performed using an ABI 7300 real-time PCR system (Applied Biosystems, Foster City, CA, USA) and TaqMan 2× PCR Universal Master Mix (Applied Biosystems). PCR conditions were as follows: 50 °C for 2 min, 95 °C for 10 min and

40 cycles of 95 °C for 15 s and 60 °C for 1 min. Primer and probe sets for relative quantification of human *IFN-β* and *CXCL10* were selected from the product list of TaqMan Gene Expression Assays (Applied Biosystems). Data are expressed as the number of copies of specific mRNA per copy of the human housekeeping glyceraldehyde 3-phosphate dehydrogenase (GAPDH) mRNA. All assays were carried out in triplicate and the results are expressed as means ± SD.

2.7. Pathogenicity of the viruses in adult mice

Five 6-week-old female ddY mice (Japan SLC Inc., Hamamatsu, Japan) were intracerebrally inoculated with 0.03 ml of 10-fold serial dilution of each strain. Mock-infected mice were inoculated with 0.03 ml of diluent (E-MEM supplemented with 5% FCS) alone. The morbidity and mortality of mice were observed for 14 dpi and 50% lethal dose (LD_{50}) of each virus was calculated by the method of Reed and Muench (1938). The mice were classified into three grades: normal, neurological symptoms (such as motor incoordination, paralysis, seizure and coma) and dead. All animal experiments were conducted in accordance with the Standards Relating to the Care and Management of Experimental Animals promulgated by Gifu University, Japan (Allowance No. 08119).

2.8. Statistical analysis

Student's *t*-test was used to determine statistical significance and *P*-values of <0.05 were considered statistically significant.

3. Results

3.1. Amino acids at positions 273 and 394 in N protein are important for evasion of activation of the RIG-I-mediated IRF-3 pathway

In order to determine the amino acid that is important for evasion of RIG-I-mediated antiviral response, first, we generated three Ni-CE mutants, CE(NiN273), CE(NiN394) and CE(NiN395) strains, in which an amino acid at position 273, 394 or 395 in N protein was replaced with that of the Ni strain, respectively (Fig. 1). To confirm viability of CE(NiN273), CE(NiN394) and CE(NiN395) strains, we checked the propagation of these Ni-CE mutants in mouse neuroblastoma NA cells as reported previously (Shimizu et al., 2007) and compared the propagation of the mutants with that of Ni, Ni-CE and CE(NiN) strains. The virus titers of Ni-CE mutants in the culture fluid ranged from 4.0×10^6 to 8.1×10^6 FFU/ml at 3 dpi, comparable to those of Ni, Ni-CE and CE(NiN) strains (Fig. 1).

Next, to ensure growth properties and expression levels of N proteins of each strain in SYM-I cells, which are known to be susceptible to rabies virus and to produce IFN-β in response to viral infection (Honda et al., 1984), we examined expression levels of N protein in SYM-I cells infected with each strain by using Western blotting (Fig. 2A). We found that the expression levels of N protein in cells infected with Ni-CE mutants were comparable to those of Ni, Ni-CE and CE(NiN) strains.

To investigate the effect of infection with these Ni-CE mutants on RIG-I-mediated IRF-3 activity, we transfected an expression plasmid encoding a dominant-negative mutant of RIG-I (RIG-IC) into human neuroblastoma SYM-I cells and then checked the IRF-3-dependent IFN-β promoter activities after infection with Ni, Ni-CE, CE(NiN) or Ni-CE mutants. In agreement with results of our previous study (Masatani et al., 2010), IRF-3-dependent IFN-β promoter activity in empty vector-transfected cells infected with Ni-CE strain was significantly higher than that in Ni- and CE(NiN)-infected cells (Fig. 2B, white bars). On the other hand, the IFN-β promoter activities in empty vector-transfected cells infected with CE(NiN273), CE(NiN394) and CE(NiN395) strains were significantly

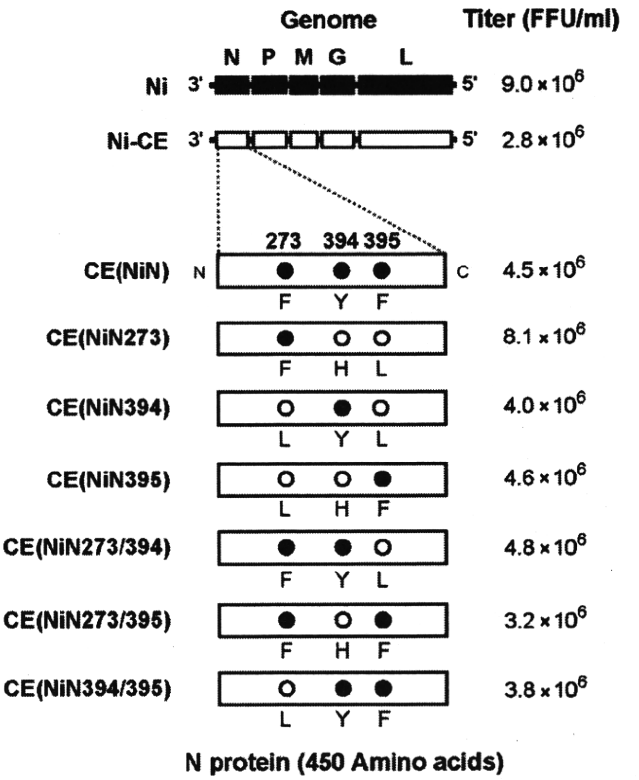

Fig. 1. Schematic diagrams of genomes and growth of Ni, Ni-CE, CE(NiN) and Ni-CE mutant strains. The filled and open circles in the N protein of each virus represent amino acids derived from Ni and Ni-CE strains, respectively. Virus titer of each virus in the supernatant of mouse neuroblastoma NA cells at 3 days post-infection is shown on the right.

higher than the activity in CE(NiN)-infected cells. Overexpression of RIG-IC significantly reduced IRF-3-dependent IFN-β promoter activity in Ni-CE-infected cells, but not in Ni- and CE(NiN)-infected cells, coinciding with results of our previous study (Masatani et al., 2010) (Fig. 2B). These results indicate that Ni-CE strain activates the RIG-I-mediated IRF-3 pathway more efficiently than do Ni and CE(NiN) strains. Meanwhile, overexpression of RIG-IC significantly reduced IFN-β promoter activity in CE(NiN273)-, CE(NiN394)- and CE(NiN395)-infected cells.

The above-described results indicate that multiple mutations in N protein are related to the evasion of activation of the host RIG-I-mediated IRF-3 pathway. Next, we generated CE(NiN273/394), CE(NiN273/395) and CE(NiN394/395) strains to identify the combination of amino acids important for the evasion of RIG-I-mediated IRF-3 activity (Fig. 1). Growth of these mutants in NA cells (Fig. 1) and expression levels of N protein in SYM-I cells infected with these mutants (Fig. 2A) were comparable to those of Ni, Ni-CE, CE(NiN) and other mutants having a single amino acid mutation. IRF-3-dependent IFN-β promoter activities in cells infected with CE(NiN273/395) and CE(NiN394/395) strains were significantly higher than those in Ni- and CE(NiN)-infected cells (Fig. 2B, white bars). On the other hand, importantly, the IFN-β promoter activity in CE(NiN273/394)-infected cells was comparable to that in CE(NiN)-infected cells. Overexpression of RIG-IC significantly reduced the IRF-3-dependent IFN-β promoter activities in CE(NiN273/395)- and CE(NiN394/395)-infected cells (Fig. 2B). However, overexpression of RIG-IC did not reduce the IFN-β promoter activity in CE(NiN273/394)-infected cells. Next, we measured the IFN-β promoter activities in wild-type RIG-I-overexpressing cells after each virus infection (Fig. 2C).

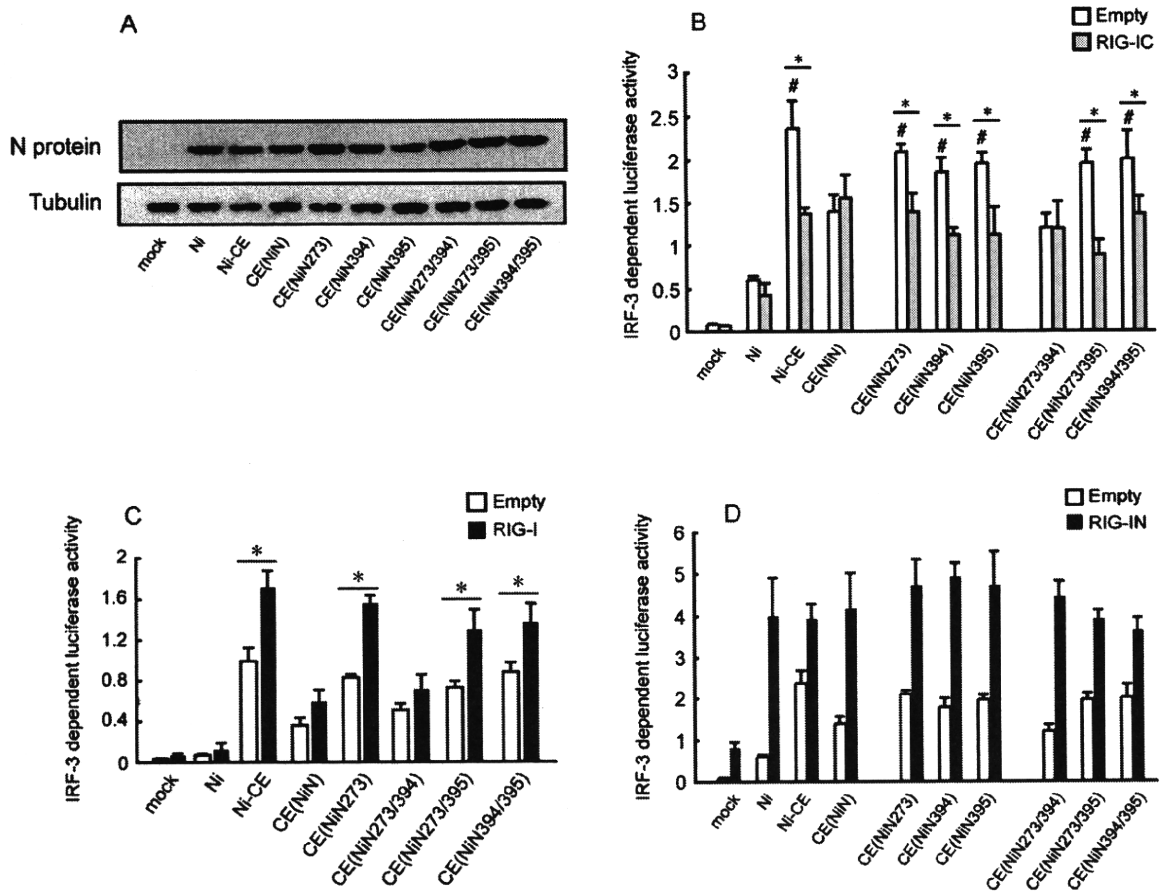

Fig. 2. Amino acids at positions 273 and 394 are important for evasion of the RIG-I-mediated IRF-3 pathway. (A) SYM-I cells were infected with Ni, Ni-CE, CE(NiN) or Ni-CE mutants at an MOI of 2. Twenty-four hours later, the cells were lysed and N protein and tubulin were detected by Western blotting. (B) SYM-I cells were inoculated, in suspension, with Ni, Ni-CE, CE(NiN) or Ni-CE mutants at an MOI of 2 and seeded. After 24 h, cells were transfected with pRL-TK, 4× IRF-3-Luc and pEF-Flag-RIG-IC or an empty vector. After 24 h, the cells were lysed and luciferase activities were measured. (C) SYM-I cells were cotransfected with pRL-TK, 4× IRF-3-Luc and 1 μg of pEF-Flag-RIG-I or an empty vector. At 24 h post-transfection, the cells were infected with Ni, Ni-CE and CE(NiN) or Ni-CE mutants at an MOI of 2 and incubated for 24 h. Then the cells were lysed and luciferase activities were measured. (D) SYM-I cells were inoculated, in suspension, with Ni, Ni-CE, CE(NiN) or Ni-CE mutants at an MOI of 2 and seeded. After 24 h, cells were transfected with pRL-TK, 4× IRF-3-Luc and pEF-Flag-RIG-IN or empty vector. After 24 h, the cells were lysed and luciferase activities were measured. Data represent firefly luciferase activity normalized to *Renilla* luciferase activity. Each bar represents the mean (±SD) of three independent replicates. *Significant difference versus empty vector-transfected cells ($P < 0.05$). #Significantly higher than the IRF-3-dependent IFN-β promoter activities in CE(NiN)-infected cells ($P < 0.05$).

Overexpression of RIG-I significantly enhanced IRF-3-dependent IFN-β promoter activity in cells infected with Ni-CE mutants except for CE(NiN273/394)-infected cells. These results indicated that amino acids at positions 273 and 394 are important to evade activation of the RIG-I-mediated IRF-3 pathway. Furthermore, we measured IRF-3-dependent IFN-β promoter activities in constitutively active mutant RIG-I (RIG-IN)-overexpressing cells after each virus infection (Fig. 2D). Expression of RIG-IN enhanced IFN-β promoter activities equivalently in Ni-, Ni-CE-, CE(NiN)- and all Ni-CE mutants-infected cells. Taken together, these results indicated that amino acids at positions 273 and 394 in N protein are important for evasion of activation of RIG-I.

3.2. Expression levels of IFN and chemokine genes in cells infected with Ni-CE mutants

Next, we examined the expression levels of *IFN-β* and *CXCL10*, which are regulated by IRF-3 (Honda and Taniguchi, 2006; Nakaya et al., 2001), in SYM-I cells infected with Ni-CE mutants (Fig. 3). In agreement with results of our previous study (Masatani et al., 2010), Ni-CE infection induced expression of *IFN-β* (Fig. 3A) and *CXCL10* genes (Fig. 3B) more efficiently than did Ni and CE(NiN) infections. Expression levels of these genes in cells infected with CE(NiN273), CE(NiN394), CE(NiN395), CE(NiN273/395) and CE(NiN394/395) strains were also significantly higher than those in CE(NiN) strain. On the other hand, importantly, expression levels of these genes in cells infected with CE(NiN273/394) strain were comparable to those in CE(NiN) strain.

3.3. Amino acids at positions 273 and 394 are also important for pathogenicity in adult mice

We next examined whether amino acids at positions 273 and 394 in N protein are important for pathogenicity in adult mice (Fig. 4). When 10^4 FFU of viruses were intracerebrally inoculated, as we expected, all mice infected with Ni and CE(NiN) strains developed neurological signs such as hyperactivity, tremor and paralysis and died within 7- and 11-dpi, respectively. In contrast, all mice infected with the Ni-CE, CE(NiN394) and CE(NiN395) strains lost weight and recovered without any neurological signs. On the other hand, CE(NiN273/395) strain had killed 40% of the mice at 12 dpi and both CE(NiN273) and CE(NiN394/395) strains had killed 20% of the mice at 10 dpi. Notably, CE(NiN273/394) strain killed all mice within 13 dpi.

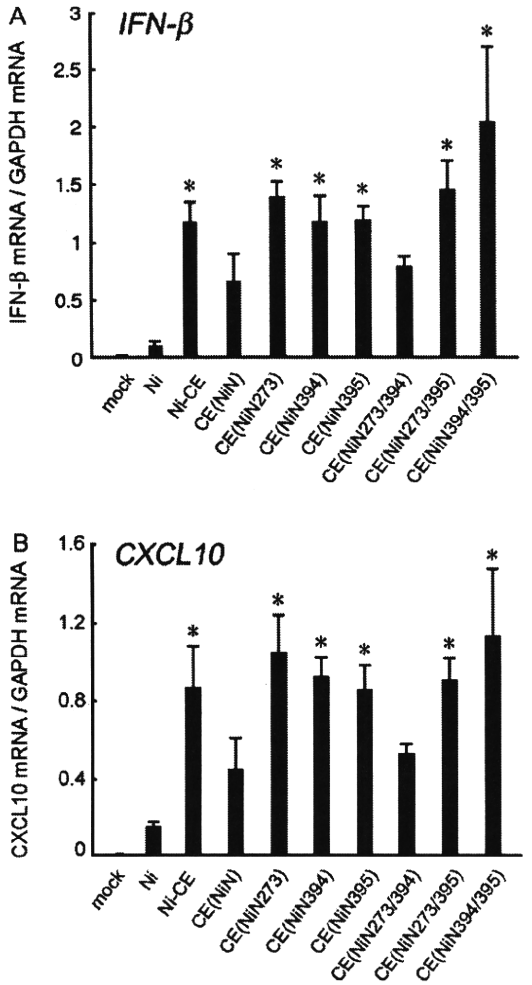

Fig. 3. Amino acids at positions 273 and 394 are important for suppression of gene expression levels of IFN/chemokine genes. SYM-I cells were mock-infected or infected with each strain at an MOI of 2. Twenty-four hours later, total cellular RNA was extracted and analyzed for expression levels of *IFN-β* (A) and *CXCL10* (B) genes by real-time PCR. Expression levels of genes were normalized to mRNA levels of *GAPDH*. Each bar represents the mean (±SD) of three independent replicates. *Significantly higher than the gene expression level of CE(NiN)-infected cells ($P < 0.05$).

The LD_{50} of Ni-CE, CE(NiN394) and CE(NiN395) strains was more than 10^5 FFU and that of CE(NiN273), CE(NiN273/395) and CE(NiN394/395) strains was ranged from 1.5×10^4 to 3.2×10^4 FFU (Table 1). On the other hand, importantly, LD_{50} of CE(NiN273/394) strain (4.2×10^2 FFU) was comparable to that of CE(NiN) strain (1.0×10^2 FFU). These results indicated that amino acids at positions 273 and 394 are also important for pathogenicity in adult mice.

4. Discussion

We previously demonstrated that the chimeric rabies virus CE(NiN) strain, which has the N gene from the virulent Ni strain in the genome of the avirulent Ni-CE strain, evades host innate immunity (Masatani et al., 2010). In this study, in order to determine which amino acids in N protein are important for the evasion, we generated six Ni-CE mutants in which one or two amino acids of N protein were replaced by those from the Ni strain in the genomic backbone of the Ni-CE strain (Fig. 1). Among these mutants, CE(NiN273/394) strain, which has substitutions at positions 273 and 394 of N protein, evaded activation of RIG-I-mediated IRF-3 activity and induction of *IFN-β* and *CXCL10* more efficiently than did the other mutants. Furthermore, in the Ni-CE mutants, CE(NiN273/394) strain showed the highest pathogenicity in adult mice. Importantly, the pathogenicity of each strain in adult mice is correlated with evasion of RIG-I-mediated host innate immunity (Table 1). While overexpression of RIG-IC significantly reduced IRF-3-dependent IFN-β promoter activities in cells infected with avirulent Ni-CE, CE(NiN394) and CE(NiN395) strains and modestly pathogenic CE(NiN273), CE(NiN273/395) and CE(NiN394/395) strains, the promoter activities in cells infected with virulent Ni, CE(NiN) and CE(NiN273/394) strains were not reduced. This correlation reinforces the relation between evasion of host RIG-I-mediated innate immunity and viral pathogenicity.

Very recently, it was reported that viral genomic RNA is a major ligand for RIG-I in cells infected with negative-sense single-stranded RNA viruses, such as influenza virus and Sendai virus (Rehwinkel et al., 2010). Since N protein of rabies virus encapsidates the viral genomic RNA (Albertini et al., 2008), it is possible that the genomic RNA encapsidated by the Ni-CE N protein is recognized more efficiently by RIG-I than the RNA with Ni or CE(NiN273/394) N protein. Previously, crystal structure analysis of N protein showed that the protein is composed of two domains, an N-terminal core domain (NTD; residues 32–233) and a C-terminal core domain (CTD; residues 236–450) (Albertini et al., 2006). It was also shown that the NTD and CTD clamp down onto the RNA and enclose it. Since both amino acids at positions 273 and 394 are located in the CTD, which is a critical part of the N protein for encapsidation (Albertini et al., 2008), these mutations may affect the N–RNA interaction and change the structure of the nucleocapsid.

Another possible mechanism by which Ni-CE and CE(NiN273/394) infection differently activate RIG-I-mediated antiviral response is that CE(NiN273/394) N protein, but not Ni-CE N protein, restricts the amount of RIG-I ligand, such as viral genomic RNA in infected cells. However, we previously showed that efficiency of viral genome replication of Ni-CE strain is comparable to that of CE(NiN) strain (Masatani et al., 2010). Therefore, it is unlikely that the amino acids at positions 273 and 394 in N protein affect the genome replication of Ni-CE and CE(NiN) strains. Notably, some studies have demonstrated that induction of type I IFN is triggered by RNA of defective-interference (DI) particles of measles virus and Sendai virus (Shingai et al., 2007; Strahle et al.,

Table 1
LD_{50}, evasion of RIG-I-mediated host antiviral response and pathogenicity in adult mice of parental/mutant viruses generated in this study.

Strain	LD_{50} (FFU)	Evasion of RIG-I-mediated host antiviral response[a]	Pathogenicity in adult mice[b]
Ni	ND[c]	+	++++
Ni-CE	$>1.0 \times 10^5$	–	–
CE(NiN)	1.0×0^2	+	+++
CE(NiN273)	2.4×10^4	–	+
CE(NiN394)	$>1.0 \times 10^5$	–	–
CE(NiN395)	$>1.0 \times 10^5$	–	–
CE(NiN273/394)	4.2×10^2	+	+++
CE(NiN273/395)	1.5×10^4	–	+
CE(NiN394/395)	3.2×10^4	–	+

[a] Evasion of RIG-I-mediated host antiviral responses was evaluated by IFN-b promoter activity inhibited by overexpression of RIG-IC in SYM-I cells infected with each virus (Fig. 2B). (–) Overexpression of RIG-IC significantly reduced IRF-3-dependent IFN-b promoter activity ($P < 0.05$); (+) Overexpression of RIG-IC did not reduce the promoter activity ($P > 0.05$).

[b] The pathogenicity was evaluated by i.c. inoculation for adult mice with 104 FFU of each virus (Fig. 4). (–) Nonlethal; (+) 20–40% of mice died within 14 dpi; (+++) all mice died within 14 dpi; (++++) all mice died within 7 dpi.

[c] Not determined in this study.

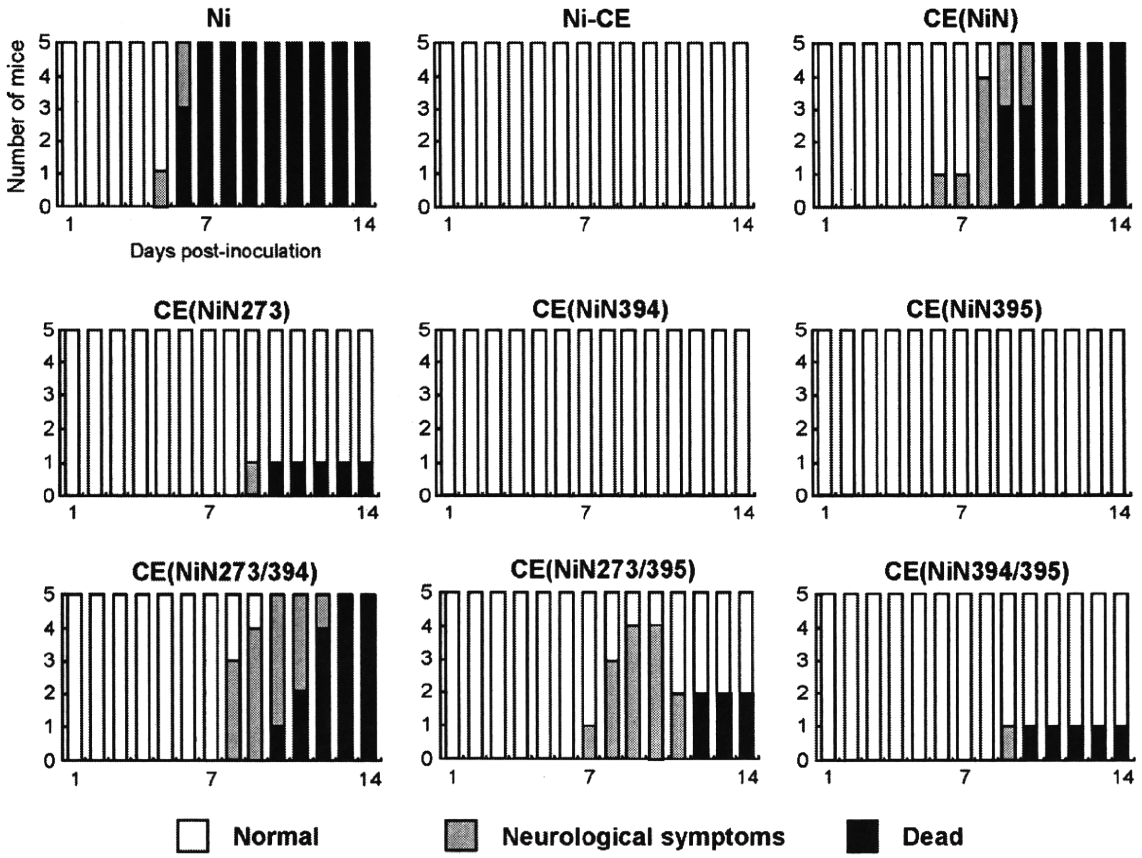

Fig. 4. Morbidity and mortality changes in adult mice inoculated intracerebrally with Ni, Ni-CE, CE(NiN) and Ni-CE mutants. Five mice per group were inoculated with 10^4 FFU of each strain. The mice were observed for neurological symptoms for 14 days and classified into three grades: normal (white), neurological symptoms (such as motor incoordination, paralysis, seizure and coma) (gray) and dead (black).

2006). Thus, it is possible that CE(NiN273/394) N protein, but not Ni-CE N protein, limits the generation of DI RNA and consequently suppresses the activation of RIG-I-mediated antiviral responses.

In conclusion, we have shown that the amino acids at positions 273 and 394 are important for evasion of RIG-I-mediated antiviral response. Furthermore, we have shown that amino acids at positions 273 and 394 in rabies virus N protein are also important for pathogenicity. This highlights the importance of evasion of RIG-I-mediated host innate immunity in viral pathogenicity.

Acknowledgements

We thank Dr. A. Kawai (Research Institute for Production and Development, Kyoto, Japan) for providing SYM-I cells. We are grateful to Dr. S. Ludwig (Westfaelische-Wilhelms University, Muenster, Germany) and Dr. T. Fujita (Kyoto University, Kyoto, Japan) for providing plasmids.

This study was partially supported by a Grant-in-Aid for Scientific Research from the Ministry of Education, Culture, Sports, Science and Technology, Japan (No. 22780261), a grant (Project Code No., I-AD14-2009-11-01) from National Veterinary Research & Quarantine Service, Ministry for Food, Agriculture, Forestry and Fisheries, Korea in 2008 and Health and Labor Sciences Research Grants from Japanese Ministry of Health, Labor and Welfare.

References

Akira, S., Uematsu, S., Takeuchi, O., 2006. Pathogen recognition and innate immunity. Cell 124, 783–801.

Albertini, A.A., Schoehn, G., Weissenhorn, W., Ruigrok, R.W., 2008. Structural aspects of rabies virus replication. Cell. Mol. Life Sci. 65, 282–294.

Albertini, A.A., Wernimont, A.K., Muziol, T., Ravelli, R.B., Clapier, C.R., Schoehn, G., Weissenhorn, W., Ruigrok, R.W., 2006. Crystal structure of the rabies virus nucleoprotein–RNA complex. Science 313, 360–363.

Daffis, S., Samuel, M.A., Keller, B.C., Gale Jr., M., Diamond, M.S., 2007. Cell-specific IRF-3 responses protect against West Nile virus infection by interferon-dependent and -independent mechanisms. PLoS Pathog. 3, e106.

Delhaye, S., Paul, S., Blakqori, G., Minet, M., Weber, F., Staeheli, P., Michiels, T., 2006. Neurons produce type I interferon during viral encephalitis. Proc. Natl. Acad. Sci. U.S.A. 103, 7835–7840.

Ehrhardt, C., Kardinal, C., Wurzer, W.J., Wolff, T., von Eichel-Streiber, C., Pleschka, S., Planz, O., Ludwig, S., 2004. Rac1 and PAK1 are upstream of IKK-epsilon and TBK-1 in the viral activation of interferon regulatory factor-3. FEBS Lett. 567, 230–238.

Finke, S., Conzelmann, K.K., 2003. Dissociation of rabies virus matrix protein functions in regulation of viral RNA synthesis and virus assembly. J. Virol. 77, 12074–12082.

Finke, S., Conzelmann, K.K., 2005. Replication strategies of rabies virus. Virus Res. 111, 120–131.

Genin, P., Algarte, M., Roof, P., Lin, R., Hiscott, J., 2000. Regulation of RANTES chemokine gene expression requires cooperativity between NF-kappa B and IFN-regulatory factor transcription factors. J. Immunol. 164, 5352–5361.

Haller, O., Kochs, G., Weber, F., 2006. The interferon response circuit: induction and suppression by pathogenic viruses. Virology 344, 119–130.

Honda, K., Taniguchi, T., 2006. IRFs: master regulators of signalling by Toll-like receptors and cytosolic pattern-recognition receptors. Nat. Rev. Immunol. 6, 644–658.

Honda, Y., Kawai, A., Matsumoto, S., 1984. Comparative studies of rabies and Sindbis virus replication in human neuroblastoma (SYM-I) cells that can produce interferon. J. Gen. Virol. 65, 1645–1653.

Hornung, V., Ellegast, J., Kim, S., Brzozka, K., Jung, A., Kato, H., Poeck, H., Akira, S., Conzelmann, K.K., Schlee, M., Endres, S., Hartmann, G., 2006. 5′-Triphosphate RNA is the ligand for RIG-I. Science 314, 994–997.

Ito, N., Takayama-Ito, M., Yamada, K., Hosokawa, J., Sugiyama, M., Minamoto, N., 2003. Improved recovery of rabies virus from cloned cDNA using a vaccinia virus-free reverse genetics system. Microbiol. Immunol. 47, 613–617.

Lefort, S., Soucy-Faulkner, A., Grandvaux, N., Flamand, L., 2007. Binding of Kaposi's sarcoma-associated herpesvirus K-bZIP to interferon-responsive factor 3 elements modulates antiviral gene expression. J. Virol. 81, 10950–10960.

Masatani, T., Ito, N., Shimizu, K., Ito, Y., Nakagawa, K., Sawaki, Y., Koyama, H., Sugiyama, M., 2010. Rabies virus nucleoprotein functions to evade activation of RIG-I-mediated antiviral response. J. Virol. 84, 4002–4012.

Mebatsion, T., Weiland, F., Conzelmann, K.K., 1999. Matrix protein of rabies virus is responsible for the assembly and budding of bullet-shaped particles and interacts with the transmembrane spike glycoprotein G. J. Virol. 73, 242–250.

Minamoto, N., Tanaka, H., Hishida, M., Goto, H., Ito, H., Naruse, S., Yamamoto, K., Sugiyama, M., Kinjo, T., Mannen, K., Mifune, K., 1994. Linear and conformation-dependent antigenic sites on the nucleoprotein of rabies virus. Microbiol. Immunol. 38, 449–455.

Nakaya, T., Sato, M., Hata, N., Asagiri, M., Suemori, H., Noguchi, S., Tanaka, N., Taniguchi, T., 2001. Gene induction pathways mediated by distinct IRFs during viral infection. Biochem. Biophys. Res. Commun. 283, 1150–1156.

Randall, R.E., Goodbourn, S., 2008. Interferons and viruses: an interplay between induction, signalling, antiviral responses and virus countermeasures. J. Gen. Virol. 89, 1–47.

Reed, L.J., Muench, H., 1938. A simple method of estimating fifty percent end points. Am. J. Hyg. 27, 493–497.

Rehwinkel, J., Reis e Sousa, C., 2010. RIGorous detection: exposing virus through RNA sensing. Science 327, 284–286.

Rehwinkel, J., Tan, C.P., Goubau, D., Schulz, O., Pichlmair, A., Bier, K., Robb, N., Vreede, F., Barclay, W., Fodor, E., Reis e Sousa, C., 2010. RIG-I detects viral genomic RNA during negative-strand RNA virus infection. Cell 140, 397–408.

Schnell, M.J., McGettigan, J.P., Wirblich, C., Papaneri, A., 2010. The cell biology of rabies virus: using stealth to reach the brain. Nat. Rev. Microbiol. 8, 51–61.

Shimizu, K., Ito, N., Mita, T., Yamada, K., Hosokawa-Muto, J., Sugiyama, M., Minamoto, N., 2007. Involvement of nucleoprotein, phosphoprotein, and matrix protein genes of rabies virus in virulence for adult mice. Virus Res. 123, 154–160.

Shingai, M., Ebihara, T., Begum, N.A., Kato, A., Honma, T., Matsumoto, K., Saito, H., Ogura, H., Matsumoto, M., Seya, T., 2007. Differential type I IFN-inducing abilities of wild-type versus vaccine strains of measles virus. J. Immunol. 179, 6123–6133.

Strahle, L., Garcin, D., Kolakofsky, D., 2006. Sendai virus defective-interfering genomes and the activation of interferon-beta. Virology 351, 101–111.

Yamada, K., Ito, N., Takayama-Ito, M., Sugiyama, M., Minamoto, N., 2006. Multigenic relation to the attenuation of rabies virus. Microbiol. Immunol. 50, 25–32.

Yoneyama, M., Kikuchi, M., Natsukawa, T., Shinobu, N., Imaizumi, T., Miyagishi, M., Taira, K., Akira, S., Fujita, T., 2004. The RNA helicase RIG-I has an essential function in double-stranded RNA-induced innate antiviral responses. Nat. Immunol. 5, 730–737.